2-2008

Doping of a One-Dimensional Mott Insulator: Photoemission and Optical Studies of Sr2Cu03+δ

Tim Kidd
Brookhaven National Laboratory

T. Valla
Brookhaven National Laboratory

See next page for additional authors

Let us know how access to this document benefits you

Recommended Citation

Authors

Tim Kidd, T. Valla, P. D. Johnson, K. W. Kim, G. D. Gu, and C. C. Homes

Doping of a one-dimensional Mott insulator: Photoemission and optical studies of $Sr_2CuO_{3+\delta}$

T. E. Kidd,[1,2,*] T. Valla,[1] P. D. Johnson,[1] K. W. Kim,[1,3] G. D. Gu,[1] and C. C. Homes[1]

[1]*Condensed Matter Physics and Materials Science Department, Brookhaven National Laboratory, Upton, New York 11973, USA*

[2]*Department of Physics, University of Northern Iowa, Cedar Falls, Iowa 50614, USA*

[3]*Department of Physics, University of Fribourg, Chemin du Musée 3, CH-1700 Fribourg, Switzerland*

Angle-resolved photoemission and optical spectroscopy are used to probe the electronic structure of the one-dimensional Mott insulator $Sr_2CuO_{3+\delta}$, both at half-filling and with small concentrations of excess oxygen doping. Spin-charge separation can be seen as evidenced by the existence of spinon and holon branches in the photoemission spectra. Optical studies reveal no significant doping dependence, while photoemission studies show a large energy shift in the spinon and holon states with respect to the main valence band states which remain nearly unaffected. The results suggest the excess dopant carriers are incorporated solely within the one-dimensional Hubbard band which is electronically isolated from the rest of the states in the system.

I. INTRODUCTION

One-dimensional (1D) Mott insulators have been studied extensively both theoretically and experimentally because of the fundamentally different excitation properties expected in 1D systems.[1] Materials with weakly interacting Cu-O chains, such as the strontium cuprate family, are a nearly ideal representation of a Heisenberg spin-1/2 chain.[2] Unlike three-dimensional systems, the elementary electronic excitations in 1D materials are not quasiparticles, but rather collective excitations carrying either spin without charge (spinons) or charge without spin (holons).[3] If created in such a system, a physical electron (or hole) decays into a pair of independent excitations. A photoemission spectrum that measures the spectral function of a physical hole in such a 1D system is therefore a broad multiparticle continuum of spinon and holon states. The boundaries of the continuum, representing one particle left at rest, may still be well defined allowing the identification of the spinon and holon branches in photoemission.[4,5] Theoretical studies predict that direct observation of separate spinon-holon branches is most easily achieved in insulating 1D materials.[6] In a 1D Mott insulator with an odd number of electrons per unit cell, these systems are insulating due to the strong electronic correlations that forbid double occupancy of sites. However, while the charge excitations are gapped, spin excitations remain gapless and form a spinon Fermi surface of their own. The gap in the charge excitations enhances the distinction between holon and spinon branches, making the boundaries more observable. Photoemission experiments have indeed indicated the presence of separate branches in 1D Mott insulators,[7] with unambiguous results achieved only recently.[8]

Doping of such 1D systems is expected to reveal further exotic properties. While doping in standard materials shifts the Fermi level of the system and is well understood, doping in Mott insulators can lead to fundamentally different physics and has been at the forefront of condensed matter research for some time. Perhaps the most well known of these effects is the emergence of unconventional superconductivity in two-dimensional (2D) cuprates with doping, creating a phase different from the antiferromagnetic insula-

tors in the undoped parent compounds. In Sr_2CuO_3, it may be possible to use doping to enhance or control some of the attractive properties which show promise for electro-optical applications.[9]

In this paper, we explore the influence of doping on the electronic structure of $Sr_2CuO_{3+\delta}$. Single-crystal samples doped with excess oxygen were found to show a significant reduction of the gap in photoemission measurements, while the optical spectra remained nearly unchanged. For the small amounts of doping used in this study, the system remained in an insulating state with no signs of any crossover to 2D behavior. The doped samples measured with photoemission also showed sharper features enabling an unambiguous determination of the spinon and holon branches in the spectra. Furthermore, only the 1D Hubbard band was strongly affected by oxygen doping as higher binding energy states in the valence band showed little changes.

II. EXPERIMENT

Large single crystals of $Sr_2CuO_{3+\delta}$ were grown using the traveling-solvent floating zone method under various oxygen pressures up to 11 bar. The resistance of doped samples was compared to undoped crystals via a simple two-probe resistance measurement using silver paint to create electrodes. Doped samples, although insulating, were more conductive, with samples grown under 11 bar oxygen pressure approximately ten times more conductive than stoichiometric samples.

The angle-resolved photoemission measurements were carried out on a high-resolution photoemission facility based on the undulator beamline U13UB at the National Synchrotron Light Source with a Scienta SES-2002 spectrometer. The combined instrumental energy resolution was set to ~25 meV. The angular resolution was better than ±0.01° translating into a momentum resolution of ±0.0025 Å^{-1} at the 15.2 eV photon energy used in this study. Samples were mounted on a liquid He cryostat and cleaved *in situ* within the ultrahigh vacuum (UHV) chamber with a base pressure less than 1×10^{-10} Torr.
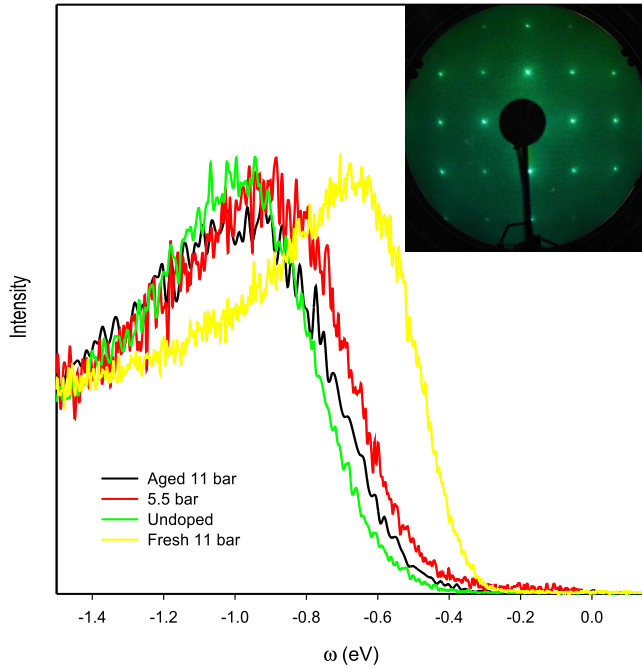
FIG. 1. (Color online) Photoemission spectra at k_F for different growth conditions of $Sr_2CuO_{3+\delta}$. Spectra were recorded at 200 K (doped) and 300 K (undoped) samples. Spectrum of the aged 11 bar sample was taken 24 h after cleaving. Inset: LEED pattern from the sample grown under 11 bar O_2 pressure.

For optical measurements, the crystals of $Sr_2CuO_{3+\delta}$ were cleaved and mounted in a dry argon atmosphere due to the sensitivity of these materials to moisture.[10] The reflectance has been measured at a near-normal angle of incidence for different polarizations over a wide frequency range ($\sim$30 to over 23 000 cm^{-1} or $\sim$3 meV to about 3 eV) on a Bruker IFS 66v/S Fourier transform spectrometer using an *in situ* evaporation technique.[11] The principle optical axes were determined from the anisotropic behavior of the phonons; a prominent infrared-active B_{2u} copper-oxygen stretching mode at $\sim$540 cm^{-1} was observed only along the chain direction (b axis) of the crystal.[12,13] The optical properties were calculated from a Kramers-Kronig analysis of the reflectance.

III. RESULTS AND DISCUSSION

A. Incorporation of dopants

While there have been several studies of polycrystalline $Sr_2CuO_{3+\delta}$ samples doped via growth at high oxygen pressures, the present study appears to be the first of oxygen-doped single crystals of the material. At high levels of doping, $Sr_2CuO_{3+\delta}$ is known to undergo a structural phase transition to a tetragonal structure with a high transition temperature superconducting ground state.[14] The single-crystal samples studied here remained insulating and retained their orthorhombic structure as determined by low energy electron diffraction (LEED), shown in the inset of Fig. 1, consistent with a study of lightly doped polycrystalline samples with δ ranging from 0.03 to 0.1 (Ref. 15).

By incorporating the excess oxygen during synthesis rather than postannealing treatments in a high oxygen pressure atmosphere, the excess oxygen is distributed homogeneously throughout the crystal. However, the surface-sensitive photoemission measurements indicated a loss of oxygen over a finite time scale. Photoemission spectra taken from doped samples that were aged in UHV were almost identical to those taken from undoped samples, as seen in Fig. 1. The lower Hubbard band shows the expected shift toward the Fermi level for hole-doped crystals grown at higher oxygen pressures. However, spectra from samples grown at even 11 bar oxygen pressure appear nearly identical to undoped crystals after aging in UHV for an extended period. This is clearly a surface effect, as the doped spectral features could be recovered by recleaving these samples in vacuum. This indicates that over a time scale significant for our measurements, the only significant loss of oxygen in the doped samples occurred very near to the sample surface. The optical measurements are less surface sensitive and reflect the bulk doping levels of the crystals.

The exact oxygen content for the samples is unknown, other than the observation that the orthorhombic structure and insulating character of the samples is consistent with that seen in a previous study of polycrystalline samples with doping levels $\delta < 0.1$;[15] this study on lightly doped polycrystalline materials suggested that the excess oxygen went into interstitial sites in the rocksalt Sr(La)O structure. Such interstitial oxygen can oxidize the Cu-O chains in the same manner as the CuO_2 planes in $La_2CuO_{4+\delta}$. In undoped samples, the chains are filled and the Fermi momentum k_F is located exactly midway between the Brillouin zone center and zone edge along the chain direction at $0.5\pi/b$. If the chains were doped by holes, k_F would be smaller. As Sr_2CuO_3 is a Mott insulator, k_F can be measured by the location of the maximum of the lower Hubbard band. The location of k_F for a 5.5 bar sample is shown in the upper panel of Fig. 2, with the full spectrum taken near k_F in the lower panel. The momentum distribution curve (MDC) is taken at a binding energy of $\omega=0.35$ eV within the gap where only the "tail" of the lower Hubbard band exists. Although the relative angle is known to a high precision, the total error of the absolute position of k_F is approximately 3% due to uncertainties in the orientation and work function of the sample. The MDC is peaked close to $0.5\pi/b$ for all samples, indicating the doping level is relatively small as the departure from half filling is within the overall uncertainty of the measurement.

As expected for hole-doped samples, the leading edge of the lower Hubbard band shifts toward the Fermi level with increased doping (Fig. 3). Examination of higher energy states reveals that these shift by far less, in contrast to both semiconductors and 2D Mott insulators, where doping generally gives rise to an overall shift in the chemical potential affecting all states equally. Furthermore, the fact that $Sr_2CuO_{3+\delta}$ remains insulating when doped contrasts strongly with 2D cuprates, where even a small concentration of doped carriers (1%–2%) induces states at the Fermi level and "metallic" in-plane transport.[16] The extra oxygen therefore appears to introduce extra hole carriers into only the charge transfer band without giving rise to a significant overall shift in the Fermi level of the system.
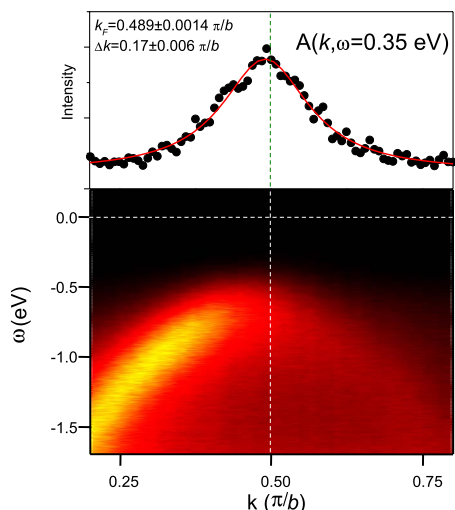
FIG. 2. (Color online) Photoemission intensity of 5.5 bar sample in the chain direction. Lower panel shows false color contour map with highest intensity in yellow. The dashed lines represent $\omega=0$ and $k=\pi/(2b)$. Upper panel represents the cross section of the same spectrum (MDC) at $\omega=-0.35$ eV. The solid line is Lorentzian fit to the data.

Charging effects will be a concern for photoemission studies in these insulating materials. Charging would cause the spectra to broaden and shift to higher binding energies, effects which would be magnified at lower temperatures and larger incident light intensities. These effects mimic some of the properties in the doped samples, where higher concentrations of hole carriers would be expected to both reduce charging effects and shift the spectra toward the Fermi level. However, it is unlikely that charging effects could account for the energy shifts to be different for different states, as seen in the present study. Further, the light intensity was varied by more than a factor of 3 with no effect on the spectra. Finally, even for samples with a gap (based on peak binding energy at k_F) greater than 0.9 eV, significant overall
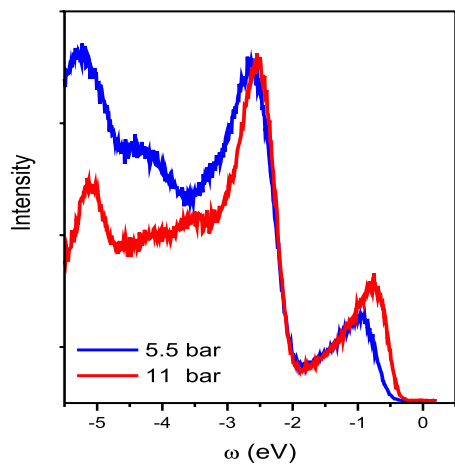

FIG. 3. (Color online) Energy distribution curves of photoemission spectra measured at room temperature and at k_F for samples grown at 11 and 5.5 bar O$_2$ pressures.

energy shifts were not seen in the samples until the temperature was reduced to less than 80 K. By limiting studies to sample temperatures of 180 K or higher, it was therefore possible to minimize the effects of charging.

Another possible source of error might be the development of a surface-photovoltage effect in the doped crystals, as is common in photoemission from semiconducting systems at low temperatures. While such an effect is consistent with the direction of shift, the peaks should all shift by a constant amount. Furthermore, the spectral shifts are independent of temperature. These results indicate the strong changes in the charge transfer band are intrinsic to the sample and do not arise from external sources.

B. Spin-charge separation

In Fig. 4(a), the photoemission intensity is plotted for the chain direction in the first Brillouin zone from an 11 bar sample taken at 180 K. In the raw data plot, there is a hint of two separate branches in the dispersion of the highest occupied state for $k<k_F$. The reduced intensity seen after the Fermi wave vector ($k>k_F$) is not unusual[7,8] and is likely due to matrix element effects which probably differ between the two halves of the Brillouin zone. Examination of the energy distribution curves (EDCs) [Fig. 4(b)] reveals a complex structure in the leading peak in the first third of the Brillouin zone. Very close to the zone center, two dispersing steplike features can be seen: a rapidly dispersing one at higher binding energies and a slowly dispersing one nearer to the Fermi level. They merge near k_F to form a single peak. These observations are consistent with earlier studies of spin charge separation. The rapidly dispersing branch is symmetric about k_F and arises from holon states, whereas the peak at lower binding energies is due to spinons and is observable only in the first half of the Brillouin zone.

Due to the overlap and breadth of the peaks in the spectra, multiple points were analyzed to extract the dispersion information. In analyzing the data, it is inappropriate to fit the states with a simple Lorentzian or Gaussian distribution. Where two distinct states can be seen, one can identify the energies where the "midpoint" of the intensity and "full-step" intensity for the steplike features, as shown in the inset of Fig. 4(c). In cases where only a single peak is present, the peak position and leading edge are plotted. The results are shown in Fig. 4(c). Both methods of analysis give nearly identical results for the dispersion, except for an offset in the energy. The measurements indicate the bandwidth for the holon branch is 1.64 eV and the spinon branch is 0.4 eV. In the t-J model, this corresponds to $t=0.82$ eV and $J=0.26$ eV, somewhat larger than estimates for an undoped system.[2,17–19] As noted earlier, the principal change in the spectra induced by increasing oxygen is the gap reduction. At the same time, the bottom of the holon branch remains at the same energy (~2.5 eV), implying that the holon bandwidth increases with oxygen doping. Examination of the gap dependence on the oxygen pressure during growth indicates $t\sim0.66$ and 0.72 eV for the undoped and 5.5 bar grown crystals, respectively. We were able to resolve the spinon state in the 5.5 bar system, but not the undoped crystals.
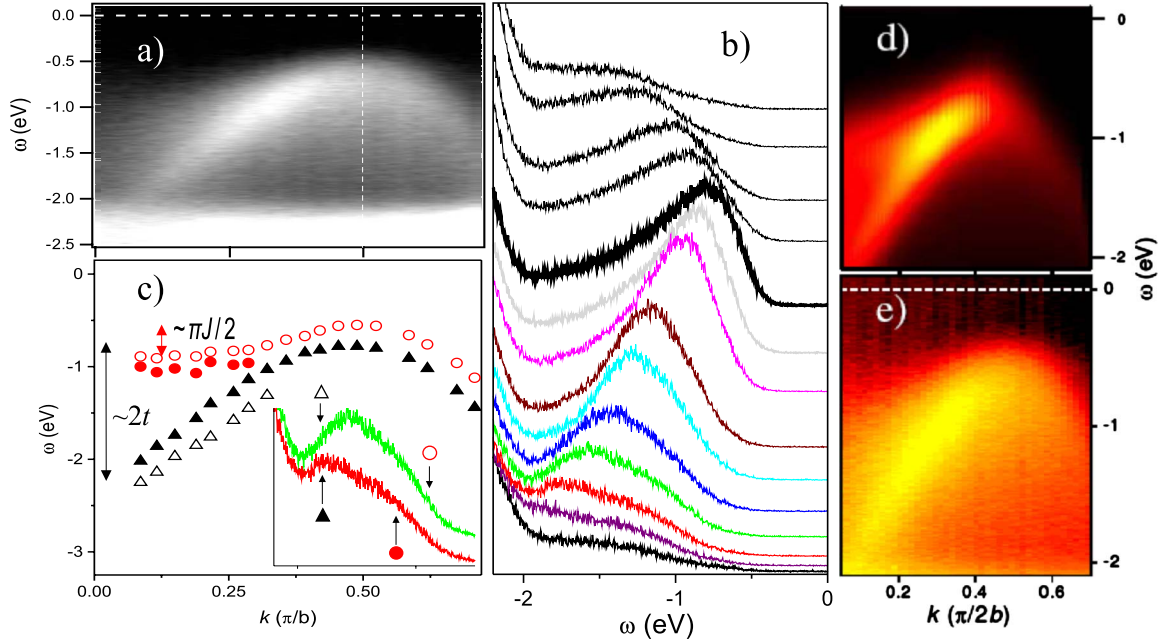
FIG. 4. (Color online) (a) Contour plot of photoemission intensity recorded at 180 K from a freshly cleaved 11 bar grown sample in the chain direction. The dashed line represents $k = \pi/(2b)$. (b) A set of corresponding EDCs for several momenta, increasing from bottom to the top. The thick spectrum corresponds to k_F. (c) Dispersion of characteristic features in the spectra from panel (b). Solid (empty) circles represent "full" ("middle") step on the upper (spinon) edge, while triangles represent corresponding features on the lower (holon) edge, as indicated in the inset for replotted third and fourth EDCs from the bottom in panel (b). (d) The simulated spectral function as explained in the text (Ref. 5). (e) The same spectrum as in (a), but with intensity on a logarithmic scale, emphasizing the spinon branch.

Compared to the 11 bar sample, J is slightly reduced in the 5.5 bar system, but within the experimental error of ± 0.5 eV.

C. Spectral broadening

In this study, as in other photoemission measurements of 1D Mott insulators, the spectra are significantly broader than would be predicted from theory.[5,6,20] In Fig. 4(d), we show a simulation of the measurements using the model 1D spectral function for a half-filled Mott insulator.[5] The spectral function is defined as

$$A(\omega, k_F + q) = -\frac{1}{\pi} \text{Im } G(\omega, k_F + q),$$

where $G(\omega, k_F + q)$ is the retarded Green's function [Eq. (23) in Ref. 5]

$$G(\omega, k_F + q) \propto \sqrt{\frac{2}{1+\alpha}} \frac{\omega + v_c q}{\sqrt{m^2 + v_c^2 q^2 - \omega^2}}$$

$$\times \left[(m + \sqrt{m^2 + v_c^2 q^2 - \omega^2})^2 \right.$$

$$\left. - \frac{1-\alpha}{1+\alpha} (\omega + v_c q)^2 \right]^{-1/2},$$

and $\alpha = v_s / v_c$. The parameters used in the simulation are $v_F k_F = 1.5$ eV and $U = 4.4$ eV for the on-site repulsion. The velocity ratio of the spinion branch spinon branch [$v_s = v_F$

$- U/(4k_F)$] to holon branch [$v_c = v_F + U/(4k_F)$] is $v_s/v_c = 0.154$, with a gap of $m = 0.65$ eV. In order to reproduce the experimental spectra, the calculated spectral function was broadened with a 0.35 eV full width at half maximum Gaussian. The agreement with the experimentally measured dispersion is excellent. However, it is unclear why such a large degree of broadening is necessary to reproduce the spectra, including the weakened intensity of the spinon state. In Fig. 4(d), a logarithmic scale of the contour plot is shown, allowing a more direct comparison of the spinon branch.

The observed asymmetry in intensity between spinon and holon branches cannot be explained in a simple one-band Hubbard model. Theories which go beyond a one-band model seem to be able to account for this apparent weakening in the signal for the spinon branch,[21] but still there exists the discrepancy of the width of the states seen in the measurement and the relatively large intensity seen within the gap. As the spinons are gapless, the "Fermi surface" they form will be broadened at finite temperatures. However, recent finite temperature calculations have shown this will affect the holon branch more strongly and cannot explain the experimental observations reported here.[6] Even the temperature dependence of the broadening is questionable. As Fig. 5 demonstrates, for our measurements ranging from 110 to 290 K, which are all less than 0.04 times the gap energy, there is almost no change in the spectral properties as a function of temperature. This indicates that whatever may be causing the broadening is already saturated by 110 K or is independent of temperature. Interestingly, a similar temperature independence for binding energies greater than $k_B T$ is reported for the cuprates.
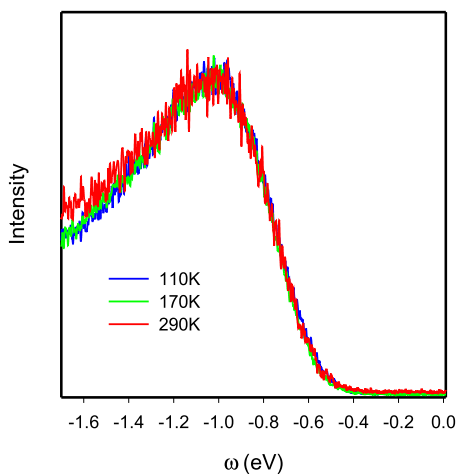
FIG. 5. (Color online) Photoemission spectra taken at k_F of the lower Hubbard band at three temperatures ranging from 110 to 290 K. Spectra were taken from a single 11 bar O_2 sample 24 h after the initial cleave to preclude any aging effects in the spectra.

The only influence on spectral width in our measurements arises from the oxygen content. As can be seen in Fig. 1, the width of the charge transfer band actually becomes slightly sharper with increased doping. This would indicate that disorder, which is the usual source of temperature-independent broadening in photoemission, is not the leading cause. It seems unlikely that adding oxygen impurities to the system would result in a better ordering of the Cu-O chains. While the source of the broadening is not clear, it should also be noted that increased doping tends to produce sharper states in 2D cuprates as compared to photoemission spectra from underdoped compounds, which may have some relation to the observations reported here. To the best of our knowledge, no model can currently explain the key features seen in the broadening of the spectra. Whatever the cause, the sharpened features seen in the doped samples allow for a better measurement of the subtle features in the electronic structure.

D. Comparison of optical and photoemission spectra

The effects of doping are clearly seen in the changes in the leading edge of the photoemission spectra, which shifts from $\Delta \simeq 0.75$ eV in the undoped sample to $\Delta \lesssim 0.5$ eV in the material grown in 11 bar of oxygen, as shown in Fig. 6(a). However, the optical properties show a surprising insensitivity to the effects of oxygen doping. The optical conductivity (or current-current correlation function) measures a two-particle correlation function that represents an integral throughout the Brillouin zone for all $q=0$ transitions,[24] while the spectral function measured in photoemission is a single-particle measurement that is resolved in both energy and momentum. As such, the conductivity is a reflection of the joint density of states and the optical gap is normally expected to be twice the gap observed in photoemission measurements.

The real part of the optical conductivity at room temperature for light polarized along the chain direction is shown in Fig. 6(b); the conductivity is effectively zero at low fre-
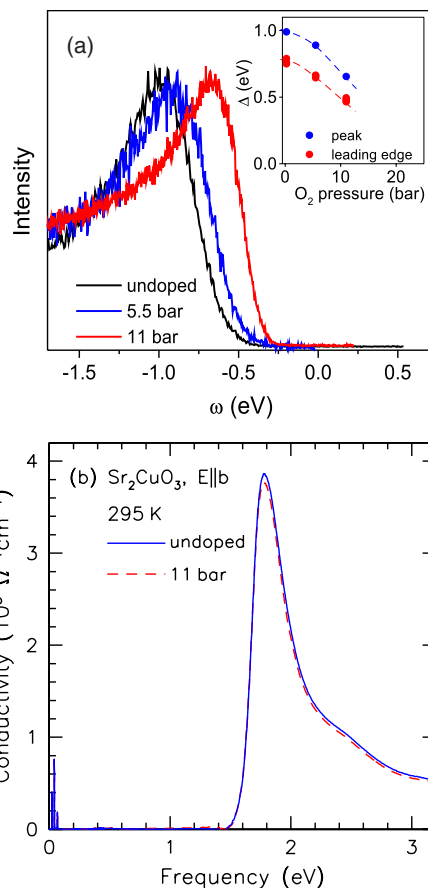

FIG. 6. (Color online) (a) Photoemission spectra at k_F for three different growth conditions of $Sr_2CuO_{3+\delta}$. Spectra were recorded at 200 K (doped) and 300 K (undoped) samples. Inset: the single-particle gap dependence on O_2 growth pressure. (b) Real part of the optical conductivity at 295 K for light polarized along the b axis (chain direction) for the undoped and 11 bar O_2 grown samples. The sharp structure at low frequency are the infrared-active lattice vibrations (Ref. 13).

quency, with a sharp onset at the optical gap of $2\Delta \simeq 1.5$ eV. The conductivity displays a strong asymmetric profile with a square root behavior above the gap that is expected for a 1D Mott-Hubbard insulator in a large-U limit.[22,23] While the optical gap in the undoped sample $2\Delta \simeq 1.5$ eV is indeed roughly twice what is observed in photoemission ($\Delta \simeq 0.75$ eV); the reduction of the leading-edge gap in photoemission studies of the doped sample of $\Delta \lesssim 0.5$ implies that the optical gap should be of the order of $2\Delta \simeq 1$ eV, whereas no change in the optical gap is observed in response to doping. In the undoped samples there is a direct transition from the charge transfer band at k_F to states at equal energy above the Fermi level. However, the reduction of the gap seen in photoemission for doped samples is not reflected in the optical measurements. The optical measurements appear to indicate that the effects of doping are constrained to a shifting of the chemical potential of the system. However, as discussed earlier (Fig. 3), doping influences on the photoemission spectra are mainly seen in the charge-transfer band, with smaller shifts seen in higher-energy states. Even if the shifts in the high-energy states

were attributed to a chemical potential shift, the optical measurement has more than enough sensitivity to detect the difference in the charge transfer gap.

It has been shown that, for many 1D systems, the optical gap can be larger than that expected from photoemission.[25] However, these effects are typically quite small in copper oxide materials and would not explain the lack of doping dependence in the optical spectra. Our results indicate that in some way the charge-transfer band undergoes a shift in energy which is decoupled from the rest of the states in the system. However, the mechanism for this energy shift remains unclear.

IV. CONCLUSIONS

We have succeeded in doping the single chain Mott insulator Sr_2CuO_3 with excess hole carriers via high-pressure oxygen growth. The doped samples remain in an insulating state with no signs of an incipient 2D structural transition, and k_F remains close to $\pi/(2b)$, indicating a very low doping level. Upon doping, the single particle gap measured in photoemission decreases, while the optical gap remains constant. This apparent contradiction appears to indicate a decoupling of the charge transfer band from other electronic states in the system. These results are inconsistent with charging or other anomalous effects from measurement and represent intrinsic properties of the material.

The doped samples provide strong evidence for spin-charge separation in the 1D $Sr_2CuO_{3+\delta}$ system. A direct analysis of the data provides an unambiguous measurement for the bandwidth of the spinon and holon branches in the system and determine the set of *t-J* parameters that agree well with earlier estimates. We are able to simulate our spectra using a theoretical 1D model with the inclusion of a simple broadening parameter. While the source of this broadening remains unclear, the doping dependence and lack of temperature dependence in our data combined with the near universality of broad features seen in other studies indicate that the large linewidths seen in photoemission studies arise from the unique properties of 1D systems that reflect their non-Fermi liquidlike character.

*tim.kidd@uni.edu

[1] S. Maekawa and T. Tohyama, Rep. Prog. Phys. **64**, 383 (2001), and references therein.

[2] A. Keren, L. P. Le, G. M. Luke, B. J. Sternlieb, W. D. Wu, Y. J. Uemura, S. Tajima, and S. Uchida, Phys. Rev. B **48**, 12926 (1993); T. Ami, M. K. Crawford, R. L. Harlow, Z. R. Wang, D. C. Johnston, Q. Huang, and R. W. Erwin, *ibid.* **51**, 5994 (1995); N. Motoyama, H. Eisaki, and S. Uchida, Phys. Rev. Lett. **76**, 3212 (1996); K. M. Kojima, Y. Fudamoto, M. Larkin, G. M. Luke, J. Merrin, B. Nachumi, Y. J. Uemura, N. Motoyama, H. Eisaki, S. Uchida, K. Yamada, Y. Endoh, S. Hosoya, B. J. Sternlieb, and G. Shirane, *ibid.* **78**, 1787 (1997).

[3] V. J. Emery, A. Luther, and I. Peschel, Phys. Rev. B **13**, 1272 (1976); E. H. Lieb and F. Y. Wu, Phys. Rev. Lett. **20**, 1445 (1968).

[4] A. Parola and S. Sorella, Phys. Rev. B **45**, 13156 (1992); S. Sorella and A. Parola, *ibid.* **57**, 6444 (1998).

[5] F. H. L. Essler and A. M. Tsvelik, Phys. Rev. B **65**, 115117 (2002).

[6] F. H. L. Essler and A. M. Tsvelik, Phys. Rev. Lett. **90**, 126401 (2003).

[7] C. Kim, A. Y. Matsuura, Z.-X. Shen, N. Motoyama, H. Eisaki, S. Uchida, T. Tohyama, and S. Maekawa, Phys. Rev. Lett. **77**, 4054 (1996); C. Kim, Z.-X. Shen, N. Motoyama, H. Eisaki, S. Uchida, T. Tohyama, and S. Maekawa, Phys. Rev. B **56**, 15589 (1997).

[8] B. J. Kim, H. Koh, E. Rotenberg, S.-J. Oh, H. Eisaki, N. Motoyama, S. Uchida, T. Tohyama, S. Maekawa, Z.-X. Shen, and C. Kim, Nat. Phys. **2**, 397 (2006).

[9] T. Ogasawara, M. Ashida, N. Motoyama, H. Eisaki, S. Uchida, Y. Tokura, H. Ghosh, A. Shukla, S. Mazumdar, and M. Kuwata-Gonokami, Phys. Rev. Lett. **85**, 2204 (2000).

[10] J. M. Hill, D. C. Johnston, and L. L. Miller, Phys. Rev. B **65**, 134428 (2002).

[11] C. C. Homes, M. Reedyk, D. A. Crandles, and T. Timusk, Appl. Opt. **32**, 2972 (1993).

[12] M. Yoshida, S. Tajima, N. Koshizuka, S. Tanaka, S. Uchida, and S. Ishibashi, Phys. Rev. B **44**, 11997 (1991).

[13] Y. S. Lee, T. W. Noh, H. S. Choi, E. J. Choi, H. Eisaki, and S. Uchida, Phys. Rev. B **62**, 5285 (2000).

[14] Z. Hiroi, M. Takano, M. Azuma, and Y. Takeda, Nature (London) **364**, 315 (1993).

[15] W. B. Archibald, J.-S. Zhou, and J. B. Goodenough, Phys. Rev. B **52**, 16101 (1995).

[16] S. Komiya, Y. Ando, X. F. Sun, and A. N. Lavrov, Phys. Rev. B **65**, 214535 (2002); S. Uchida, T. Ido, H. Takagi, T. Arima, Y. Tokura, and S. Tajima, *ibid.* **43**, 7942 (1991); M. Dumm, Seiki Komiya, Yoichi Ando, and D. N. Basov, Phys. Rev. Lett. **91**, 077004 (2003); T. Yoshida, X. J. Zhou, T. Sasagawa, W. L. Yang, P. V. Bogdanov, A. Lanzara, Z. Hussain, T. Mizokawa, A. Fujimori, H. Eisaki, Z.-X. Shen, T. Kakeshita, and S. Uchida, *ibid.* **91**, 027001 (2003).

[17] H. Suzuura, H. Yasuhara, A. Furusaki, N. Nagaosa, and Y. Tokura, Phys. Rev. Lett. **76**, 2579 (1996); R. Neudert, M. Knupfer, M. S. Golden, J. Fink, W. Stephan, K. Penc, N. Motoyama, H. Eisaki, and S. Uchida, *ibid.* **81**, 657 (1998).

[18] Young-June Kim, J. P. Hill, H. Benthien, F. H. L. Essler, E. Jeckelmann, H. S. Choi, T. W. Noh, N. Motoyama, K. M. Kojima, S. Uchida, D. Casa, and T. Gog, Phys. Rev. Lett. **92**, 137402 (2004).

[19] I. A. Zaliznyak, H. Woo, T. G. Perring, C. L. Broholm, C. D. Frost, and H. Takagi, Phys. Rev. Lett. **93**, 087202 (2004).

[20] H. Matsueda, N. Bulut, T. Tohyama, and S. Maekawa, Phys. Rev. B **72**, 075136 (2005).

[21] K. Penc and W. Stephan, Phys. Rev. B **62**, 12707 (2000).

[22] E. Jeckelmann, F. Gebhard, and F. H. L. Essler, Phys. Rev. Lett. **85**, 3910 (2000).

[23] Z. V. Popović, V. A. Ivanov, M. J. Konstantinović, A. Cantarero, J. Martínez-Pastor, D. Olguín, M. I. Alonso, M. Garriga, O. P. Khuong, A. Vietkin, and V. V. Moshchalkov, Phys. Rev. B **63**, 165105 (2001).

[24] R. Kubo, J. Phys. Soc. Jpn. **12**, 570 (1957); D. A. Greenwood, Proc. Phys. Soc. London **71**, 585 (1958).

[25] Norikazu Tomita and Keiichiro Nasu, Phys. Rev. B **64**, 125118 (2001); Solid State Commun. **111**, 175 (1999).